RSC Advances

PAPER

View Article Online
View Journal | View Issue

Cite this: *RSC Adv.*, 2019, **9**, 36103

Fe_3O_4@BNPs@SiO_2–SO_3H as a highly chemoselective heterogeneous magnetic nanocatalyst for the oxidation of sulfides to sulfoxides or sulfones

Mohammad Ghanbari Kermanshahi[a] and Kiumars Bahrami *[ab]

Received 9th August 2019
Accepted 17th October 2019

DOI: 10.1039/c9ra06221a

rsc.li/rsc-advances

To achieve green chemistry goals and also to reduce the cost of catalysts as well as to avoid producing toxic wastes and show the importance of separation and recycling of catalysts from the reaction medium, in this work, we describe the preparation and characterization of magnetic acidic boehmite nanoparticles as a heterogeneous catalyst, which is called Fe_3O_4@BNPs@SiO_2–SO_3H. This catalyst works efficiently in the selective oxidation of sulfides to sulfoxides or sulfones in the presence of H_2O_2 as a green oxidant. It can easily be separated from the reaction medium by using an external magnet and it was recycled 6 times without loss of magnetic catalytic properties.

Introduction

Selective oxidation of sulfides into sulfoxides or sulfones is one of the most significant and fascinating reactions in organic chemistry[1] because they are valuable synthetic intermediates for the pharmaceutical and chemical industry.[2] A literature survey revealed that sulfoxide derivatives are reported to have an important role in enzyme activation,[3] are used as solvents,[4] and have a wide range of pharmacological activity.[5] Also, sulfones and sulfoxides have many applications in the fields of organic synthesis,[6] agrochemistry[7] and medical syntheses.[8]

Recently, researchers have developed numerous techniques for the oxidation of sulfoxides and sulfones.[9] Among possible oxidation pathways, the use of hydrogen peroxide for oxidation of sulfides is more preferable[10] because it has several pros like low-price, secure storage, being readily accessible, and soluble in a large number of organic solvents as well as in water, and producing water as a green by-product.[11–14] In recent years, many catalysts including homogeneous and heterogeneous ones for oxidation of sulfides have been announced. Although these methods have a lot of potential, the reactions suffer from low yields, long run times and poor catalyst recovery, and consume too much oxidant in comparison with substrates.[15]

One of the features of homogeneous catalysts is that they can be dissolved in the reaction medium. Although solubility in homogeneous catalytic systems leads to enhancement of active sites and increasing catalytic activity, it also causes poor recovery and low reusability.

Most of the time separation of homogeneous catalysts is a problem, especially when toxic and noble metals are used. For this reason, the use of heterogeneous catalysts is proposed as a better route, because they can be easily separated from the reaction medium.[15] But, two issues of heterogeneous catalytic systems include a loss of activity and their selectivity towards homogeneous catalytic systems.[16] However, the use of nano-scale supports can be very beneficial by increasing the active sites of heterogeneous catalysts.[17]

In the past few decades, a wide range of materials have been used as catalytic supports. Graphene,[18] carbon nanotubes,[19] zeolite,[20] MOF-5,[21] and also some nanoparticles like TiO_2 NPs[22] are included among these. However, in most cases, special conditions are needed to produce these nanoparticles, such as high temperature and inert gases. Boehmite nanoparticles are considered as one of the most suitable, stable and recyclable materials due to their high mechanical and thermal stability, availability, low cost of raw materials, high surface area (>120 $m^2\ g^{-1}$), and green properties.[23,24] Many uses of boehmite have been reported in recent years, some of which include use as an absorbent, ceramic enhancer, catalyst, vaccine assistant, cosmetic product, and infrequently a support for heterogeneous catalysts.[25,26] Boehmite nanoparticles can be easily synthesized in an aqueous medium using NaOH and $Al(NO_3)_3 \cdot 9H_2O$ at appropriate conditions and room temperature.[27] The aluminum oxide-hydroxide boehmite (γ-AlOOH) mineral is a component of aluminum ore bauxite which has a surface full of hydroxyl groups.[24,28]

As a result of the disadvantages mentioned in previous researches and in continuation to our reported works in this field[29] and the use of heterogeneous nanocatalysts in organic

[a]*Nanoscience and Nanotechnology Research Center (NNRC), Razi University, Kermanshah 67149-67346, Iran. E-mail: kbahrami2@hotmail.com; k.bahrami@razi.ac.ir; Fax: +98 83 34274559*

[b]*Department of Organic Chemistry, Faculty of Chemistry, Razi University, Kermanshah 67149-67346, Iran*

reactions,[30] in this study we introduced a novel type of acidic catalyst based on a magnetic core–shell heterogeneous catalyst which is called Fe_3O_4@BNPs@SiO_2–SO_3H. These magnetic catalysts not only show high efficiency and selectivity in oxidation of sulfides but also can be separated and recovered efficiently from the reaction medium by simply applying external magnetic fields (Scheme 1). Preparation of Fe_3O_4@BNPs@SiO_2–SO_3H is shown in Scheme 2.

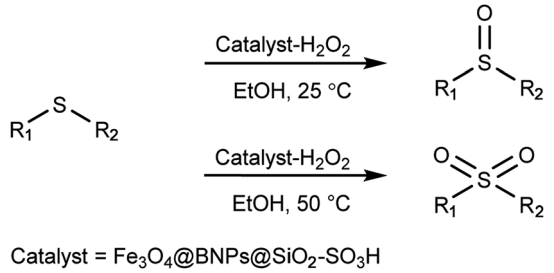

Scheme 1 Oxidation of sulfides to sulfoxides and sulfones.

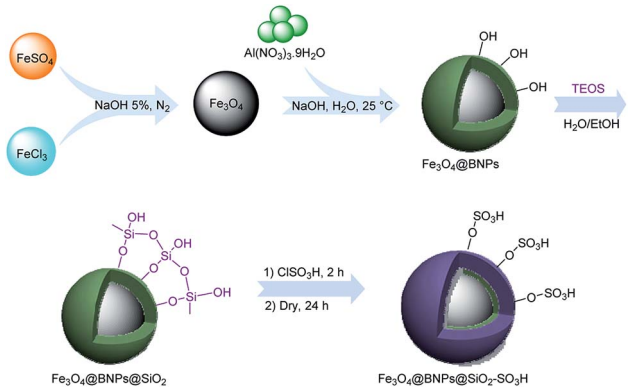

Scheme 2 Preparation of Fe_3O_4@BNPs@SiO_2–SO_3H as a magnetic acidic nanocatalyst.

Experimental

Materials were purchased from Merck and Fluka and were used without any additional purification. All reactions were monitored by TLC. Melting points were determined using a Stuart Scientific SMP2 apparatus. FT-IR spectra were determined with a PerkinElmer 683 instrument. ^{1}H NMR and ^{13}C NMR spectra were recorded with a Bruker (300 MHz) spectrometer in $CDCl_3$ as solvent. TGA was carried out with a STA PT-1000 Linseis instrument (Germany) under air atmosphere at a heating rate of 10 °C min^{-1}. FESEM and EDX measurements were performed using a TESCAN- MIRA3 operated at 26 kV with an electron gun filament of tungsten. TEM images were carried out with a Zeiss-EM10C (Germany) operating at 100 kV with samples on a formvar 300 mesh carbon-coated Cu grid. XRD patterns were obtained using a STOE STADI-P diffractometer (Cu K-α1 radiation wavelength = 1.54060 Å).

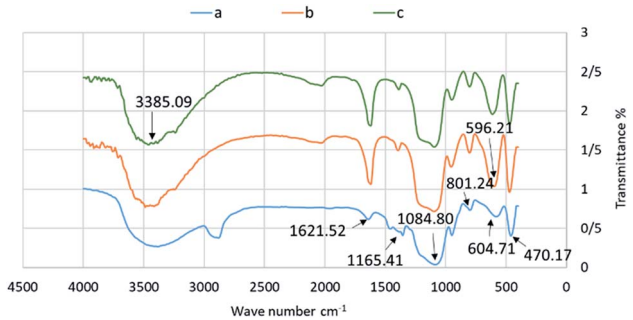

Fig. 1 FT-IR spectra of (a) boehmite nanoparticles (b) Fe_3O_4@BNPs@SiO_2 and (c) Fe_3O_4@BNPs@SiO_2–SO_3H.

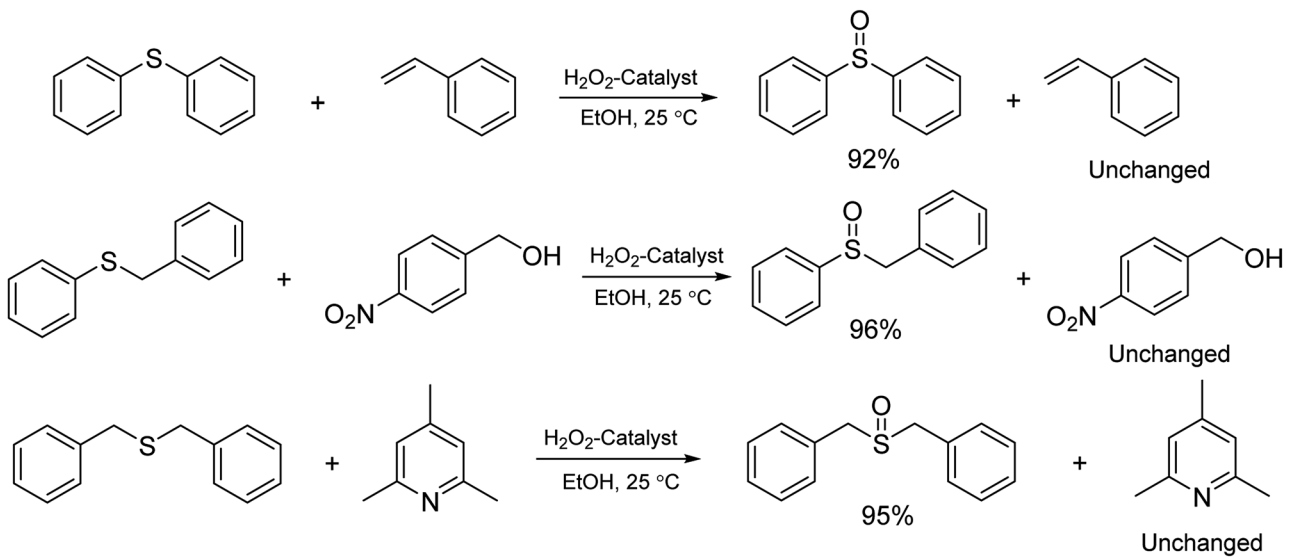

Scheme 3 Reagents and conditions: molar ratio of substrates to H_2O_2 (1 : 1 : 3) in the presence of 0.075 g of catalyst in EtOH at 25 °C.

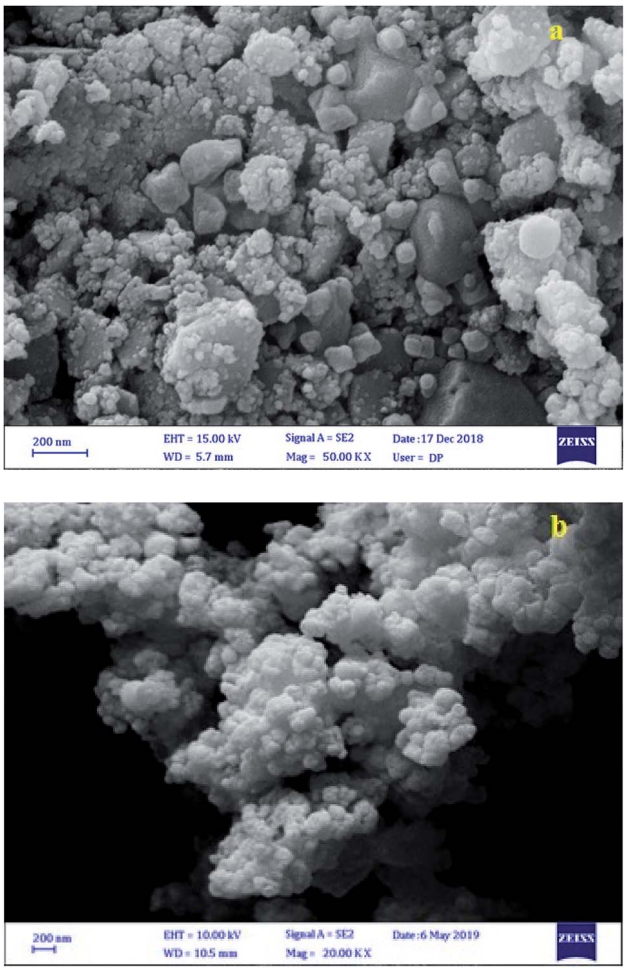

Fig. 2 FESEM images of (a) Fe_3O_4@BNPs and (b) Fe_3O_4@BNPs@SiO_2–SO_3H.

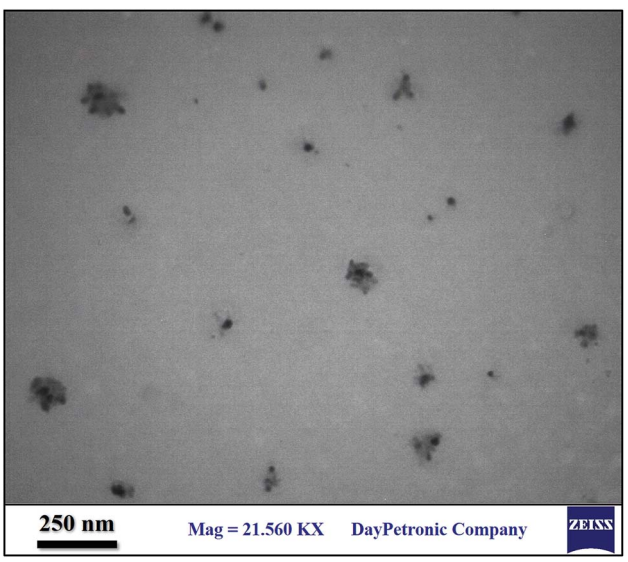

Fig. 3 TEM image of Fe_3O_4@BNPs@SiO_2–SO_3H.

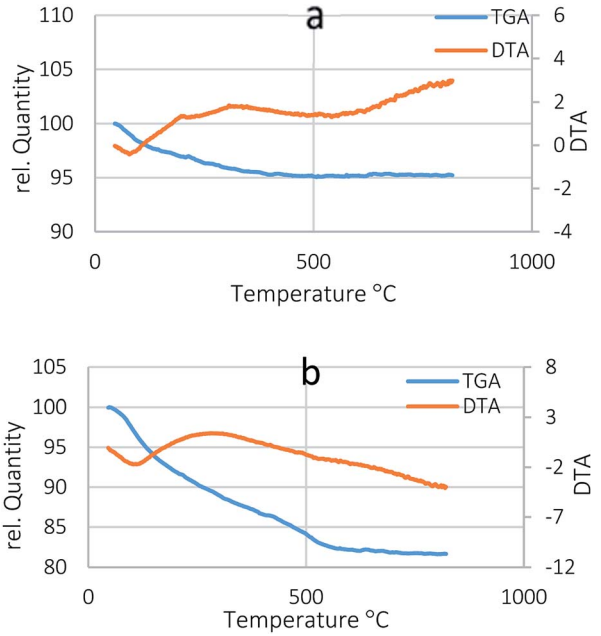

Fig. 4 TGA-DTA curve of (a) Fe_3O_4@BNPs and (b) Fe_3O_4@BNPs@SiO_2–OSO_3H.

General procedure to produce sulfoxides

To a mixture of sulfides (1 mmol) and Fe_3O_4@BNPs@SiO_2–SO_3H (0.075 g, 0.7 mmol) in ethanol (2 mL) at 25 °C was added 30% aqueous H_2O_2 (0.3 mL). The progress of the reaction was monitored by TLC (EtOAc/*n*-hexane = 2/8). After completion of the reaction, the magnetic catalyst was separated by an external magnet and washed with ethanol, then the product was extracted with EtOAc (4 × 5 mL). The organic layer was dried over anhydrous magnesium sulfate, and evaporated to afford the sulfoxides in good yields (90–98%).

General procedure to produce sulfones

Sulfides (1 mmol) were added to a mixture of 30% H_2O_2 (0.4 mL) and Fe_3O_4@BNPs@SiO_2–SO_3H (0.1 g, 0.1 mmol) in ethanol (2 mL) and the mixture was then stirred at 50 °C for the time specified. The progress of a reaction was monitored by TLC (EtOAc/*n*-hexane = 2/8). After completion of the reaction the

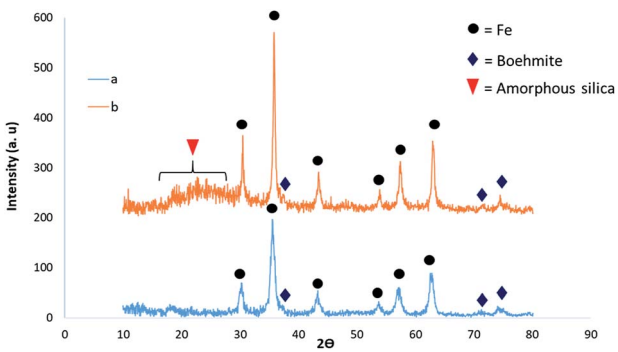

Fig. 5 XRD patterns of (a) Fe_3O_4@BNPs and (b) Fe_3O_4@BNPs@SiO_2–SO_3H.

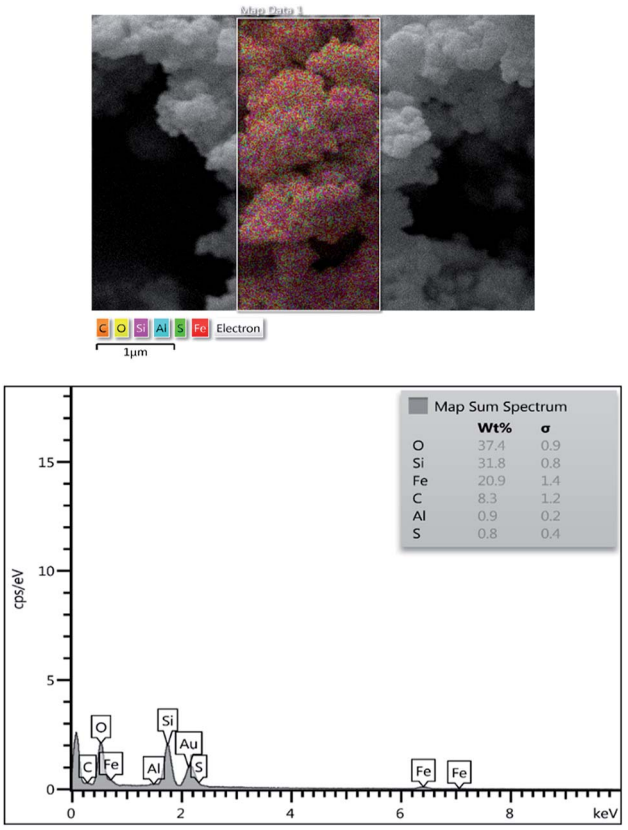

Fig. 6 EDX pattern of Fe_3O_4@BNPs@SiO_2–SO_3H.

catalyst was separated from the reaction mixture by an external magnet and washed with ethanol. Next, the residue was extracted with EtOAc (4 × 5 mL) and after that the organic layer was dried over anhydrous magnesium sulfate. Eventually, by evaporation the organic solvent sulfones were obtained in satisfactory yields (90–98%).

Preparation of Fe_3O_4@BNPs@SiO_2–SO_3H

First, a mixture of $FeCl_3 \cdot 6H_2O$ (1.55 g) and $FeSO_4 \cdot 7H_2O$ (1.05 g) in deionized water (25 mL) was magnetically stirred for 3 min at room temperature under N_2 atmosphere. Afterwards, 25 mL NaOH (5%) was added very slowly into the mixture under vigorous stirring. The resulting black mixture was continuously stirred for 2 h at 90 °C under N_2 atmosphere. After that, the mixture was allowed to cool at room temperature and then Fe_3O_4 NPs was separated by using an external magnet and washed several times with deionized water and kept in an oven at 50 °C for 24 h. In the next steps, Fe_3O_4 NPs (1 g) was dispersed in a solution of $Al(NO_3)_3 \cdot 9H_2O$ (1 g) in deionized water (25 mL); then, a solution of 0.649 g of NaOH in 10 mL of distilled water was added to the mixture drop by drop under vigorous stirring. After that the mixture was sonicated in an ultrasonic bath for 3 h at 25 °C. Finally, the produced Fe_3O_4@BNPs was separated

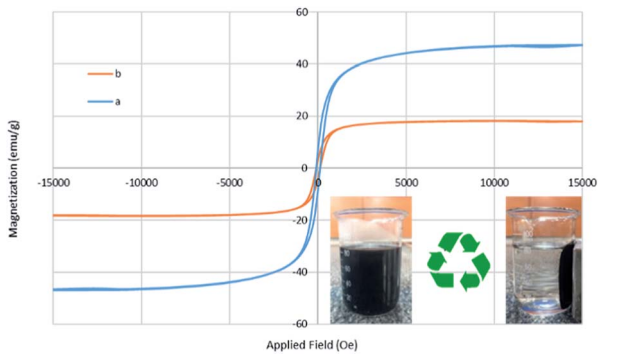

Fig. 7 VSM analysis of (a) Fe_3O_4@BNPs (b) Fe_3O_4@BNPs@SiO_2–SO_3H.

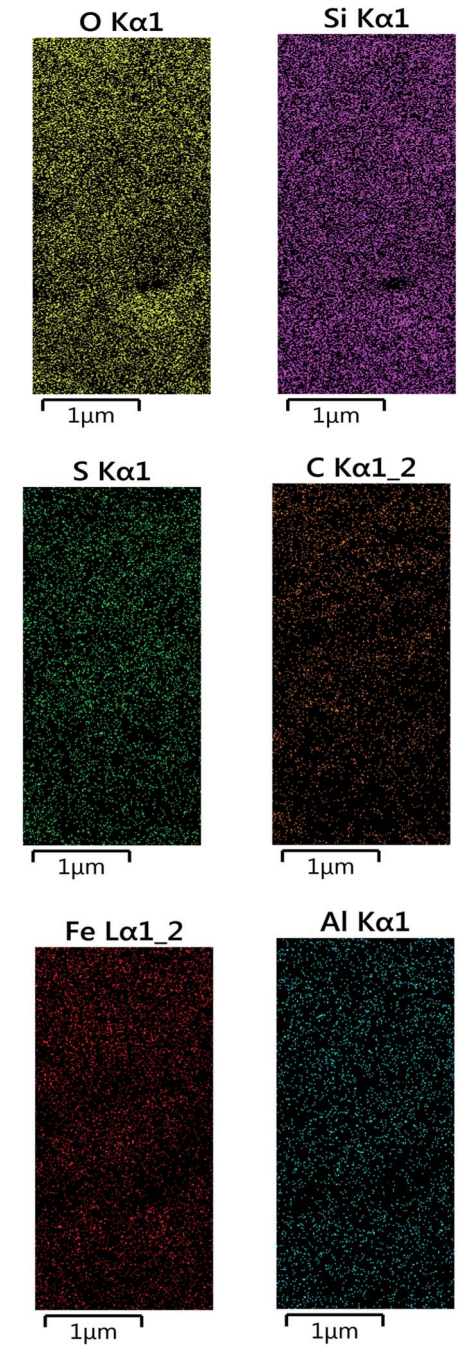

Fig. 8 Mapping pattern of Fe_3O_4@BNPs@SiO_2–SO_3H.

with an external magnet and washed with ethanol three times and dried in an oven at 60 °C for 2 h.[27,31]

Fe_3O_4@BNPs (0.5 g) was dispersed in water (5 mL) and ethanol (25 mL) in an ultrasonic bath for 30 min. Under continuous stirring, PEG (2.68 g), ammonia solution (5 mL) and TEOS (1 mL) were respectively added into the suspension, and continuously reacted for 38 h at room temperature. Then the obtained Fe_3O_4@BNPs@SiO_2 was separated by using an external magnet and washed with ethanol and distilled water and the obtained Fe_3O_4@BNPs@SiO_2 was dried at room temperature.

The obtained Fe_3O_4@BNPs@SiO_2 (0.5 g) was dispersed in dry CH_2Cl_2 (5 mL) by sonication for 30 min. Chlorosulfonic acid (0.75 mL) was added dropwise over a period of 30 min and the mixture was stirred for 4 h at room temperature. The resulting Fe_3O_4@BNPs@SiO_2–SO_3H was separated by using an external magnet and washed several times with dry CH_2Cl_2 and methanol and CH_2Cl_2 respectively to remove the unreacted materials. The final product was dried at room temperature overnight (Scheme 3).

Results and discussion

After preparation of the catalyst, the Fe_3O_4@BNPs-SiO_2–SO_3H was extensively studied with techniques such as Fourier transform infrared spectroscopy (FT-IR), transmission electron microscopy (TEM), field emission scanning electron microscopy (FESEM), thermogravimetric analysis (TGA), energy-dispersive X-ray spectroscopy (EDX), X-ray diffraction spectroscopy (XRD), vibrating-sample magnetometer (VSM) and pH analysis. Synthetic steps for preparation of the catalyst are shown in Scheme 2.

A. Ghorbani-Choghamarani and co-workers reported boehmite silica sulfuric acid for oxidation of sulfides to sulfoxides with H_2O_2 as an oxidant at room temperature.[32] It was found that in comparison with this same study, our studies led to enhancement in the selectivity and caused a gain products in high yields (90–98%) with shorter reaction times (5–45 min). Also, as a result of our work this magnetic nanocatalyst can easily be separated from the reaction medium in the shortest time possible.

The FT-IR technique was used to affirm the connection of various functional groups on a catalyst's surface. As seen in the IR spectrum of initial boehmite (Fig. 1a), the three frequencies appearing in the 470.17, 604.71 and 801.24 cm^{-1} regions are related to the Al–O stretching frequency. Also, OH···OH hydrogen bonds between layers of the boehmite nanoparticles at 1084.80 and 1165.41 cm^{-1}, and a nitrate impurity or bending vibration of O–H at 1621.52 cm^{-1} also appeared. In the Fe_3O_4@BNPs@SiO_2 IR spectrum (Fig. 1b), all of the stretching vibrations of the boehmite nanoparticles are seen with a slight displacement and the stretching frequency of Fe–O is seen at 596.21 cm^{-1}. In the FT-IR spectrum of the final catalyst, absorption bands due to hydroxyl groups at 3385.09 cm^{-1}, Al–O at 470.52 and 802.96 cm^{-1}, –Si–O at 949.28 cm^{-1} and –nitrate impurities at 1621.52 cm^{-1} were identified. Also the band at 1096.38 cm^{-1} corresponds to OH···OH hydrogen bonds between layers of boehmite. And, the bands observed at 577.15 cm^{-1} can be attributed to the Fe–O stretching frequency. After sulfonation of the Fe_3O_4@BNPs, a broad adsorption bond appeared in the 3200–3600 cm^{-1} range (Fig. 1c).[27]

FESEM was applied to study and confirm the structure and morphology of the synthesized catalysts. As Fig. 2a shows, the particles are nearly spherical with an average diameter of 30–45 nm and uniformly scattered. After acidification of the Fe_3O_4@BNPs, the morphology of the particles was preserved (Fig. 2b).

TEM was used to determine the exact size of the particles which was 20–40 nm (Fig. 3). According to TEM images, BNPs are shells, and Fe_3O_4 nanoparticles are cores.

TGA was used to study thermal behaviours of the nanocatalysts in oxidative (air) media. TGA curves for BNPs@Fe_3O_4 and acidic magnetic boehmite are shown in Fig. 4a and b. The TGA curve for BNPs@Fe_3O_4 only showed about 5% weight loss which displays

Table 1 Effect of amount of H_2O_2, Fe_3O_4@BNPs@SiO_2–SO_3H and type of solvent on oxidation of sulfides

Entry	30% H_2O_2 (mmol)	Catalyst (g)	t (min)/T (°C)	Solvent	Yield (%)	
					Sulfoxides	Sulfones
1	2	—	12 h/RT	EtOH	20	—
2	2	0.025	10/RT	EtOH	50	—
3	2	0.05	10/RT	EtOH	70	—
4	2	0.075	5/RT	EtOH	90	—
5	3	0.075	2/RT	EtOH	98	—
6	4	—	24 h/50°	EtOH	—	60
7	3	0.075	2/RT	Toluene	40	—
8	3	0.075	2/RT	H_2O	60	10
9	3	0.075	2/RT	CH_3CN	80	15
10	3	0.075	2/RT	DMF	85	10
11	3	0.05	20/50°	EtOH	—	60
12	3	0.075	15/50°	EtOH	—	80
13	3	0.1	10/50°	EtOH	—	90
14	4	0.1	10/50°	EtOH	—	98
15	4	0.1	10/RT	EtOH	60	20

Table 2 Oxidation of sulfides in presence of Fe_3O_4@BNPs-SiO_2–SO_3H with H_2O_2 in ethanol

		Sulfoxides[a]			Sulfones[b]		
Entry	Substrate	Time (min)	Yield (%)	MP[ref.]	Time (min)	Yield (%)	MP[ref.]
1	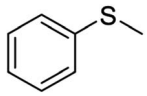	5	94	29–30[38]	10	92	83–85[39]
2	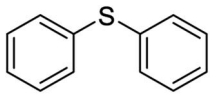	5	98	69–71[38]	10	98	125–126[26]
3	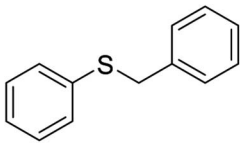	2	98	120–121[40]	10	94	146–148[41]
4	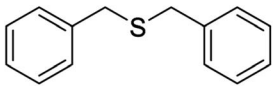	8	98	135–136[38]	15	96	149–151[26]
5	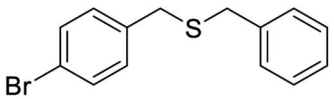	10	95	137[42]	20	95	175–177[43]
6	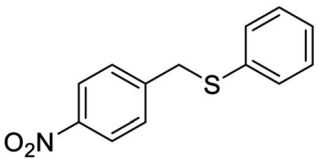	20	92	162[42]	45	96	203–205[42]
7		10	95	Oil[44]	25	90	25–28[45]
8	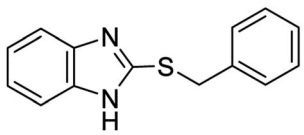	10	94	171[46]	30	96	212–214[43]
9	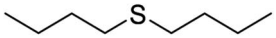	10	96	30[47]	20	96	44–46[1]
10	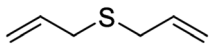	10	94	Oil[46]	20	92	Oil[1]
11	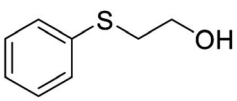	15	92	151–152[48]	30	90	Oil[1]
12	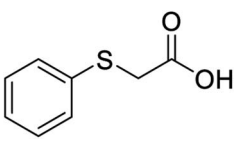	20	92	110–111[43]	40	90	110–112[42]
13	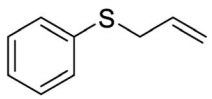	10	92	Oil[49]	25	92	Oil[50]
14	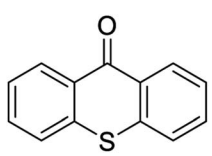	10	94	201[51]	20	94	185–187[42]

[a] Reaction conditions: sulfide (1 mmol), H_2O_2 (0.3 mL), catalyst (0.075 g) at 25 °C in EtOH. [b] Reaction conditions: sulfide (1 mmol), H_2O_2 (0.4 mL), catalyst (0.1 g) at 50 °C in EtOH.

thermal stability of the magnetic boehmite. In Fig. 4b and a gradual and subcutaneous weight loss (~13%) occurred between 50 to 400 °C, which is related to the removal of water, organic solvent, TEOS and acid groups from the catalyst's surface. A second weigh loss of ~5% occurred from 400–600 °C, and is related to the boehmite phase transformation to γ-alumina.[33,34]

To analyze the crystalline structure of the synthesized catalysts, an XRD technique was used (Fig. 5). The XRD pattern also contains peaks at 2θ values of 30.62° (220), 35.67° (311), 54.42, 57.82° (511) and 63.42° (440), which agree with the cubic structure of Fe_3O_4 NPs[35] (Fig. 5a). It is worth noting that the structure of the catalyst was maintained after modification of Fe_3O_4@BNPs with silica where some peaks at 2θ = 20–27 are related to the amorphous silica and peaks at 2θ values of 31.82° (110), 44.72° (131) and 55.25° (151) can verify the existence of boehmite[36] (Fig. 5b). An increase in peak intensities in the XRD pattern could be due to the increase in average of particle size from 16.56 nm in magnetic boehmite to 29.55 nm in the final catalyst (after silica coating on the boehmite as well as added sulfonate groups).[37]

Elemental analysis of the Fe_3O_4@BNPs@SiO_2–SO_3H was investigated by EDX where the presence of ^{1}Fe, Si, C, O, Al and S in the catalyst confirmed the successful synthesis of Fe_3O_4@BNPs@SiO_2–SO_3H (Fig. 6).

VSM analysis showed superparamagnetic behavior of the prepared Fe_3O_4@BNPs and Fe_3O_4@BNPs@SiO_2–SO_3H in Fig. 7. It can be seen that the saturation magnetization values of Fe_3O_4@BNPs and Fe_3O_4@BNPs@SiO_2–SO_3H were 42.52 and 18.21 emu g^{-1}, respectively. Functionalization of the catalyst's surface reduces its magnetic properties, but the magnetic properties of the final catalyst are still significant.

Another analysis used to confirm the existence and distribution of elements in the catalyst's structures was a mapping technique (Fig. 8) and it displayed very well all of the elements in the Fe_3O_4@BNPs@SiO_2–SO_3H structure.

Catalytic studies

To investigate effects of various variables on an oxidation reaction, we selected as a model the reaction of benzyl phenyl sulfide with H_2O_2 in the presence of Fe_3O_4@BNPs@SiO_2–SO_3H, an acidic heterogeneous catalyst in ethanol. For this purpose, factors such as solvent, amount of catalyst, amount of H_2O_2 and temperature were evaluated. At first, the model reaction was carried out in the absence of the catalyst, which after a long time formed only 20% of the sulfoxide (Table 1, entry 1).

After that, we focused on the effects of different catalyst amounts on the yields and the reaction time. Catalytic activity of Fe_3O_4@BNPs@SiO_2–SO_3H in the oxidation of various sulfides was examined with oxidation of benzyl phenyl sulfide (1 mmol) using 30% H_2O_2 in the presence of 0.025, 0.05, 0.075 and 0.1 g of Fe_3O_4@BNPs@SiO_2–SO_3H in ethanol at room temperature and under vigorous stirring until the reaction was complete (as observed by TLC). The best yield for sulfoxide (98%) was obtained in the presence of 0.075 g of catalyst, and further oxidation of the sulfoxide to its sulfone was achieved with 0.1 g of catalyst (98%) (Table 1, entry 14). Different solvents such as acetonitrile, toluene, water, ethanol and DMF also were studied and the best results were obtained in ethanol (Table 1, entry 5).

In addition, the next important factor that affected the yield and reaction time, as well as reaction selectivity, was the amount of H_2O_2. The optimum amount of H_2O_2 was 3 mmol for sulfoxide formation and 4 mmol for sulfone preparation (Table 1, entries 5 and 14).

In the following studies, the effect of temperature was considered. It is interesting to note that by controlling the amount of H_2O_2, the product will be changed. It was observed that the sulfoxide yield was reduced at 50 °C (Table 1, entry 6). It should be noted that for the oxidation of sulfide to sulfone, the best result was achieved at 50 °C (Table 1, entry 14).

The generality and scope of this protocol was assessed for the oxidation of various sulfides with H_2O_2 in the presence of Fe_3O_4@BNPs@SiO_2–SO_3H and the results are listed in Table 2. As shown in Table 2, Fe_3O_4@BNPs@SiO_2–SO_3H effectively catalyzed the oxidation reaction of sulfides bearing both electron-donating or electron-withdrawing groups with H_2O_2 (3 mmol) to afford desired products in excellent yields (92–98%) and short times (5–20 min) in EtOH. With allylic sulfides only the sulfur atom was oxidized (Table 2, entries 10, and 13). Furthermore, in the presence of alcohol, carboxyl and ketone groups could not intervene with the production derived from oxidation of sulfides (Table 2, entries 11, 12 and 14). As expected, oxidation of sulfides to sulfoxides required lower reaction times (Table 2). And as can be seen in Table 2, oxidation reactions of sulfides to sulfones in the presence of 0.1 g of the catalyst required more H_2O_2 (4 mmol) and higher reaction times (10–40 min) in EtOH at 50 °C.

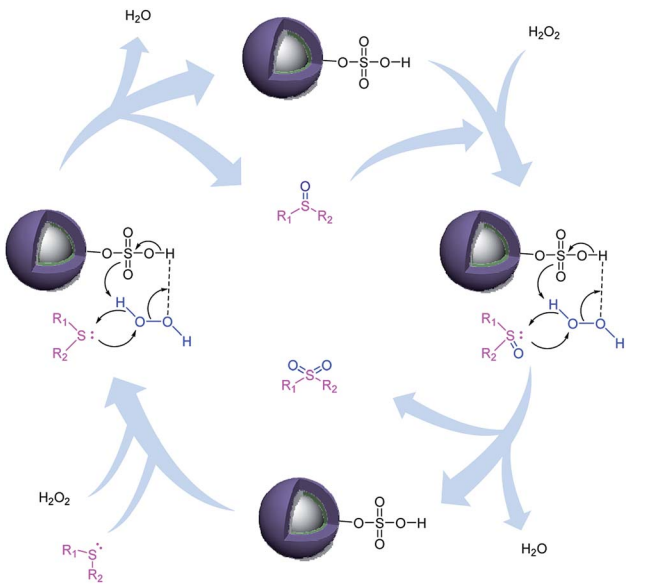

Scheme 4 Proposed mechanism for the oxidation of sulfides to sulfoxides or sulfones in the presence of Fe_3O_4@BNPs@SiO_2–SO_3H with H_2O_2 as a green oxidant.

Table 3 Comparison of present methodology with literature data for the synthesis of benzyl phenyl sulfoxide and sulfone

Entry	Product	Conditions[ref.]	Time (min)	Yield (%)
1	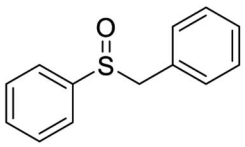	H_2O_2/Fe_3O_4@SiO_2-FeQ_3/H_2O/rt[52]	90	94
2		SBA-15-SA/H_2O/rt[53]	15	98
3		H_2O_2/SBA-15-Pr-SO_3H/CH_3CN/40 °C[54]	10	98
4		H_2O_2/Fe_3O_4@SSA/H_2O/rt[55]	5	85
5		H_2O_2/Fe_3O_4-Salen of Cu(II)/EtOH/60 °C[56]	6 h	98
6		This work	2	98
7	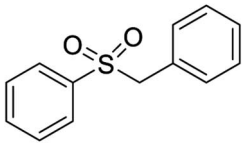	H_2O_2/MWCNTs-COOH/solvent-free/rt[57]	10 h	94
8		H_2O_2/AGO/CH_3CN/rt[58]	2 h	83
9		H_2O_2/Mo132-MimAM/H_2O/rt[59]	60	98
10		H_2O_2/SAPTPA40/CH_3CN/70 °C[60]	5.5 h	70
11		This work	10	94

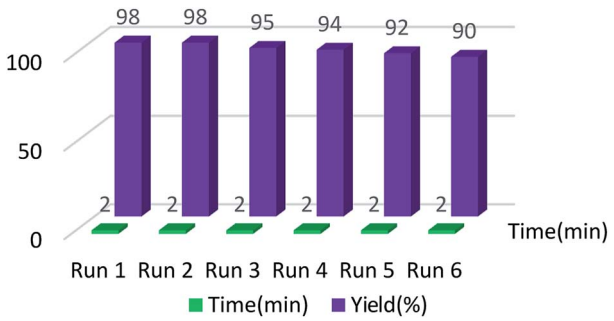

Fig. 9 Reusability of Fe_3O_4@BNPs@SiO_2–SO_3H in oxidation of benzyl phenyl sulfide to the corresponding sulfoxide.

It is important to note that the reaction time was higher in the presence of sulfides with electron-withdrawing groups such as nitro (Table 2, entry 6). With great pleasure, we saw tetrahydrothiophene and 2-(benzylthio)-1*H*-benzo[*d*]imidazole as cyclic aliphatic and heterocycle sulfides produced the corresponding products in excellent yields (Table 2, entries 7 and 8). We also accomplished several competitive reactions to show the chemoselectivity of the presented method.

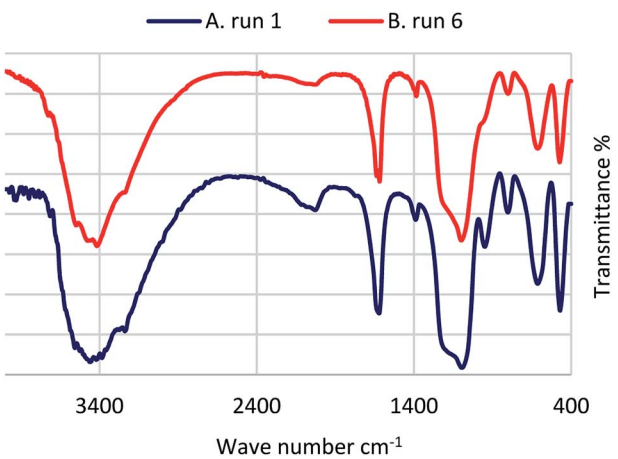

Fig. 10 FT-IR spectra of the catalyst after one run and after six runs.

According to the results of our study, the reaction tolerates sensitive functional groups such as alkenes, alcohols, and pyridine, and only the sulfur atom is selectively oxidized (Scheme 3). A detailed mechanism for the oxidation of sulfides has been proposed which includes the interaction between the catalyst and hydrogen peroxide. The OH moiety of the catalyst forms a hydrogen bond with hydrogen peroxide which increases the electrophilic ability of a peroxy oxygen atom of hydrogen peroxide and assists the leaving group (H_2O) in departing from the reaction intermediate through

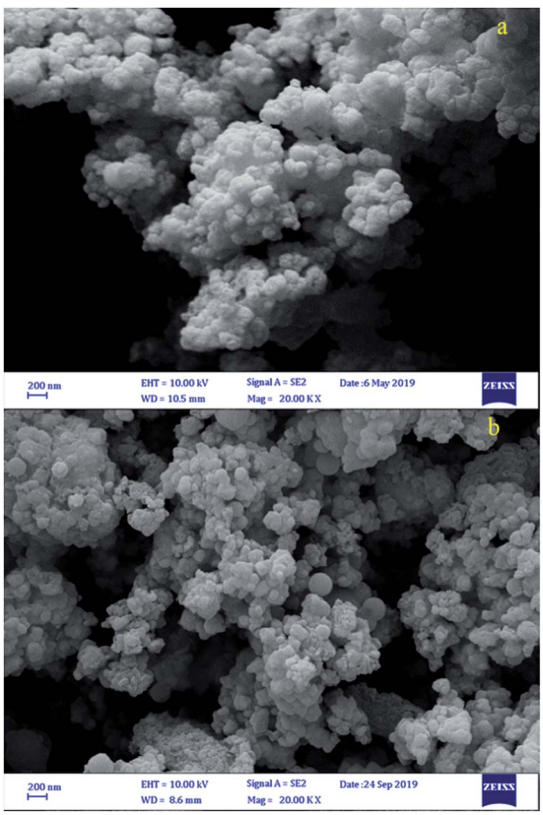

Fig. 11 FESEM images of (a) fresh Fe_3O_4@BNPs@SiO_2–SO_3H and (b) Fe_3O_4@BNPs@SiO_2–SO_3H after reuse 6 times.

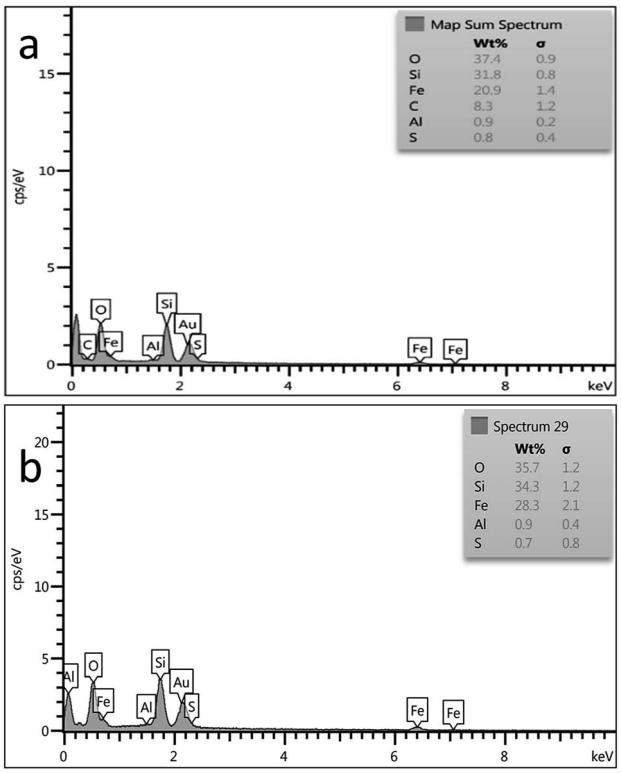

Fig. 12 EDS spectrum of (a) fresh Fe_3O_4@BNPs@SiO_2–SO_3H and (b) Fe_3O_4@BNPs@SiO_2–SO_3H after reuse 6 times.

nucleophilic attacks by sulfur atom form sulfide and sulfoxide (Scheme 4).

A comparison of the efficiency of this procedure with some previous similar methods is summarized in Table 3. The results demonstrate that this method is superior to some previously reported methods in terms of yields and times.

Reusability of the catalyst

Considering the importance of recovering catalysts from an economics view and reducing environmental pollution, scientists today are trying to synthesize renewable and green heterogeneous catalysts. In this regard, we checked the reusability of the Fe_3O_4@BNPs@SiO_2–SO_3H. The catalyst was easily isolated from the reaction media using an external magnet and washed twice with ethanol and dried for the subsequent run. Remarkably, recycling studies affirmed the thermal and chemical stability and recyclability of the catalyst. It is noteworthy that the catalyst was used during six runs (Fig. 9).

In order to check the stability of the catalyst, after reuse 6 times it was separated and analysed using FT-IR, SEM and EDS. As can be seen, data were comparable with those of the fresh catalyst (Fig. 10–12).

Conclusions

In summary, we synthesized green and stable acidic heterogeneous magnetic BNPs (Fe_3O_4@BNPs@SiO_2–SO_3H) and used them for the oxidation of sulfides to both sulfoxides and sulfones in EtOH. Here, various sulfides reacted with both electron-donating and -withdrawing groups, but sulfides reacting with withdrawing groups took longer times and gave smaller yields. The above-mentioned nanocatalyst showed high catalytic activity for the sulfide oxidation. The advantages of this protocol include low reaction times, high yields, the convenience of separating the catalyst from the reaction media, relatively inexpensive and available raw materials, the use of a green solvent, high acidity and catalyst recovery for at least 6 reuses without a dramatic drop in catalytic properties.

Conflicts of interest

There are no conflicts to declare.

Acknowledgements

We are thankful to the Razi University Research Council for partial support of this work.

Notes and references

1 K. Sato, M. Hyodo, M. Aoki, X.-Q. Zheng and R. Noyori, *Tetrahedron*, 2001, **57**, 2469–2476.
2 N. Fukuda and T. Ikemoto, *J. Org. Chem.*, 2010, **75**, 4629–4631.
3 S. E. Martín and L. I. Rossi, *Tetrahedron Lett.*, 2001, **42**, 7147–7151.
4 L. FIELD, *Synthesis*, 1978, **1978**, 713–740.
5 R. V. Kupwade, *Chem. Rev.*, 2019, **1**, 99–113.
6 N. S. Simpkins, *Sulphones in organic synthesis*, Elsevier, 2013.
7 B. Welz, *Spectrochim. Acta, Part B*, 1999, **54**, 2081–2094.
8 S. Takamuku and P. Jannasch, *Macromolecules*, 2012, **45**, 6538–6546.
9 J. K. Fink, *High Performance Polymers*, William Andrew Publishing, Norwich, NY, 2008, pp. 1–68.
10 H. Zhang and G. Wang, *Tetrahedron Lett.*, 2014, **55**, 56–58.
11 I. W. C. E. Arends and R. A. Sheldon, *Modern Oxidation Methods*, ed. J.-E. Bäckvall, Wiley-VCH, Weinheim, 2004, pp. 83–118.
12 Y. Kon, T. Yokoi, M. Yoshioka, Y. Uesaka, H. Kujira, K. Sato and T. Tatsumi, *Tetrahedron Lett.*, 2013, **54**, 4918–4921.
13 M. Kirihara, J. Yamamoto, T. Noguchi, A. Itou, S. Naito and Y. Hirai, *Tetrahedron*, 2009, **65**, 10477–10484.
14 R. Rahimi, A. A. Tehrani, M. A. Fard, B. M. M. Sadegh and H. R. Khavasi, *Catal. Commun.*, 2009, **11**, 232–235.
15 V. Polshettiwar, R. Luque, A. Fihri, H. Zhu, M. Bouhrara and J.-M. Basset, *Chem. Rev.*, 2011, **111**, 3036–3075.
16 K. Bahrami, M. M. Khodaei and M. Roostaei, *New J. Chem.*, 2014, **38**, 5515–5520.
17 Y. Zhu, L. P. Stubbs, F. Ho, R. Liu, C. P. Ship, J. A. Maguire and N. S. Hosmane, *ChemCatChem*, 2010, **2**, 365–374.
18 E. Antolini, *Appl. Catal., B*, 2012, **123**, 52–68.
19 X. Wang, W. Li, Z. Chen, M. Waje and Y. Yan, *J. Power Sources*, 2006, **158**, 154–159.

20 M. Hellinger, H. W. Carvalho, S. Baier, D. Wang, W. Kleist and J.-D. Grunwaldt, *Appl. Catal., A*, 2015, **490**, 181–192.
21 S. Opelt, S. Türk, E. Dietzsch, A. Henschel, S. Kaskel and E. Klemm, *Catal. Commun.*, 2008, **9**, 1286–1290.
22 A. Bharathi, S. M. Roopan, A. Kajbafvala, R. Padmaja, M. Darsana and G. N. Kumari, *Chin. Chem. Lett.*, 2014, **25**, 324–326.
23 V. Vatanpour, S. S. Madaeni, L. Rajabi, S. Zinadini and A. A. Derakhshan, *J. Membr. Sci.*, 2012, **401**, 132–143.
24 Z. Wu, Y. Mao, M. Song, X. Yin and M. Zhang, *Catal. Commun.*, 2013, **32**, 52–57.
25 L. Rajabi and A. Derakhshan, *Sci. Adv. Mater.*, 2010, **2**, 163–172.
26 K. Bahrami and M. Khodamorady, *Appl. Organomet. Chem.*, 2018, **32**, e4553.
27 A. Ghorbani-Choghamarani and B. Tahmasbi, *New J. Chem*, 2016, **40**, 1205–1212.
28 M. B. Gholivand, G. Malekzadeh and A. A. Derakhshan, *Sens. Actuators, B*, 2014, **201**, 378–386.
29 (*a*) K. Bahrami, M. M. Khodaei and M. Sheikh Arabi, *J. Org. Chem.*, 2010, **75**, 6208–6213; (*b*) K. Bahrami, *Tetrahedron Lett.*, 2006, **47**, 2009–2012; (*c*) M. M. Khodaei, K. Bahrami and M. Khedri, *Can. J. Chem.*, 2007, **85**, 7–11; (*d*) M. M. Khodaei, K. Bahrami and A. Karimi, *Synthesis*, 2008, 1682–1684; (*e*) K. Bahrami and M. Khodamorady, *Appl. Organomet. Chem.*, 2018, **32**, e4553; (*f*) K. Bahrami, M. M. Khodaei and S. Sohrabnezhad, *Tetrahedron Lett.*, 2011, **52**, 6420–6423.
30 (*a*) K. Bahrami, M. M. Khodaei and F. S. Meibodi, *Appl. Organomet. Chem.*, 2017, **31**, e3627; (*b*) K. Bahrami, M. M. Khodaei and M. Roostaei, *New J. Chem.*, 2014, **38**, 5515–5520; (*c*) K. Bahrami and S. Nakhjiri Kamrani, *Appl. Organomet. Chem.*, 2018, **32**, e4102; (*d*) K. Bahrami and M. Bakhtiarian, *ChemistrySelect*, 2018, **3**, 10875–10880; (*e*) K. Bahrami and M. Khodamorady, *Catal. Lett.*, 2019, **149**, 688–698; (*f*) K. Bahrami and Z. Karami, *J. Exp. Nanosci.*, 2018, **13**, 272–283; (*g*) K. Bahrami and H. Targhan, *Appl. Organomet. Chem.*, 2019, **33**, e4842; (*h*) H. Targhan, A. Hassanpour and K. Bahrami, *Appl. Organomet. Chem.*, 2019, **33**, e5121; (*i*) K. Bahrami and M. Sheikh Arabi, *New J. Chem.*, 2016, **40**, 3447–3455.
31 A. Mohammadinezhad and B. Akhlaghinia, *Green Chem.*, 2017, **19**, 5625–5641.
32 A. Ghorbani-Choghamarani, M. Hajjami, B. Tahmasbi and N. Noori, *J. Iran. Chem. Soc.*, 2016, **13**, 2193–2202.
33 A. Ghorbani-Choghamarani, P. Moradi and B. Tahmasbi, *RSC Adv.*, 2016, **6**, 56638–56646.
34 T. Bell, J. M. Gonzalez-Carballo, R. Tooze and L. Torrente-Murciano, *J. Mater. Chem. A*, 2015, **3**, 6196–6201.
35 J. Park, K. An, Y. Hwang, J.-G. Park, H.-J. Noh, J.-Y. Kim, J.-H. Park, N.-M. Hwang and T. Hyeon, *Nat. Mater.*, 2004, **3**, 891.
36 J. Safari and Z. Zarnegar, *J. Mol. Catal. A: Chem.*, 2013, **379**, 269–276.
37 M. A. Karimi and M. Kafi, *Arabian J. Chem.*, 2015, **8**, 812–820.
38 N. J. Leonard and C. R. Johnson, *J. Org. Chem.*, 1962, **27**, 282–284.
39 C. Yang, Q. Jin, H. Zhang, J. Liao, J. Zhu, B. Yu and J. Deng, *Green Chem.*, 2009, **11**, 1401–1405.
40 M. H. Ali, D. R. Leach and C. E. Schmitz, *Synth. Commun.*, 1998, **28**, 2969–2981.
41 H. Veisi, F. H. Eshbala, S. Hemmati and M. Baghayeri, *RSC Adv.*, 2015, **5**, 10152–10158.
42 K. Bahrami, *Tetrahedron Lett.*, 2006, **47**, 2009–2012.
43 K. Bahrami, M. M. Khodaei and M. Sheikh Arabi, *J. Org. Chem.*, 2010, **75**, 6208–6213.
44 A. Fabretti, F. Ghelfi, R. Grandi and U. M. Pagnoni, *Synth. Commun.*, 1994, **24**, 2393–2398.
45 D. Greig, M. Hall, C. Hammond, B. Hickey, H. Ho, M. A. Howson, M. Walker, N. Wiser and D. Wright, *J. Magn. Magn. Mater.*, 1992, **110**, L239–L246.
46 E. Rafiee, I. M. Baltork, S. Tangestaninejad, A. Azad and S. Moinee, *ýZ. Naturforsch. B Chem. Sci*, 2006, **61**, 601–606.
47 M. M. Khodaei, K. Bahrami and A. Karimi, *Synthesis*, 2008, **2008**, 1682–1684.
48 M. M. Lakouraj, M. Tajbakhsh and H. Tashakkorian, *Lett. Org. Chem.*, 2007, **4**, 75–79.
49 K. Bahrami, M. M. Khodaei, B. H. Yousefi and M. S. Arabi, *Tetrahedron Lett.*, 2010, **51**, 6939–6941.
50 M. M. Khodaei, K. Bahrami and M. Khedri, *Can. J. Chem.*, 2007, **85**, 7–11.
51 M. H. Ali and S. Stricklin, *Synth. Commun.*, 2006, **36**, 1779–1786.
52 S. Rostamnia, B. Gholipour, X. Liu, Y. Wang and H. Arandiyan, *J. Colloid Interface Sci.*, 2018, **511**, 447–455.
53 E. Doustkhah and S. Rostamnia, *Mater. Chem. Phys.*, 2016, **177**, 229–235.
54 K. Bahrami, M. M. Khodaei and P. Fattahpour, *Catal. Sci. Technol.*, 2011, **1**, 389–393.
55 A. Rostami, A. Ghorbani-Choghamarani, B. Tahmasbi, F. Sharifi, Y. Navasi and D. Moradi, *J. Saudi Chem. Soc.*, 2017, **21**, 399–407.
56 A. Ghorbani-Choghamarani, B. Ghasemi, Z. Safari and G. Azadi, *Catal. Commun.*, 2015, **60**, 70–75.
57 H. Veisi, F. H. Eshbala, S. Hemmati and M. Baghayeri, *RSC Adv.*, 2015, **5**, 10152–10158.
58 G. Abdi, A. Alizadeh and M. Khodaei, *Mater. Chem. Phys.*, 2017, **201**, 323–330.
59 R. Fareghi-Alamdari, N. Zekri, A. J. Moghadam and M. R. Farsani, *Catal. Commun.*, 2017, **98**, 71–75.
60 R. Frenzel, D. Morales, G. Romanelli, G. Sathicq, M. Blanco and L. Pizzio, *J. Mol. Catal. A: Chem.*, 2016, **420**, 124–133.

